Inorg. Chem. **2003**, *42*, 1681–1687

Inorganic Chemistry

Article

Reaction of (μ-Oxo)diiron(III) Core with CO_2 in *N*-Methylimidazole: Formation of Mono(μ-carboxylato)(μ-oxo)diiron(III) Complexes with *N*-Methylimidazole as Ligands

Dana S. Marlin,[†] **Marilyn M. Olmstead,**[‡] **and Pradip K. Mascharak***,[†]

Department of Chemistry and Biochemistry, University of California, Santa Cruz, California 95064, and Department of Chemistry, University of California, Davis, California 95616

Received October 14, 2002

Several iron(III) complexes with *N*-methylimidazole (*N*-MeIm) as the ligand have been synthesized by using *N*-MeIm as the solvent. Under anaerobic conditions, $[Fe(N\text{-MeIm})_6](ClO_4)_3$ (**1**) reacts with stoichiometric amounts of water in *N*-MeIm to afford the (μ-oxo)diiron(III) complex, $[Fe_2(\mu\text{-O})(N\text{-MeIm})_{10}](ClO_4)_4$ (**3**). Exposure of a solution of **3** in *N*-MeIm to stoichiometric and excess CO_2 gives rise to the (μ-oxo)(μ-carboxylato)diiron(III) species $[Fe_2(\mu\text{-O})(\mu\text{-HCO}_2)(N\text{-MeIm})_8](ClO_4)_3$ (**4**) and the methyl carbonate complex $[Fe_2(\mu\text{-O})(\mu\text{-CH}_3OCO_2)(N\text{-MeIm})_8](ClO_4)_3$ (**5**), respectively. Formation of the formato-bridged complex **4** upon fixation of CO_2 by **3** in *N*-MeIm is unprecedentated. Methyl transfer from *N*-MeIm to a bicarbonato-bridged (μ-oxo)diiron(III) intermediate appears to give rise to **5**. Complex **3** is a good starting material for the synthesis of (μ-oxo)mono(μ-carboxylato)diiron(III) species $[Fe_2(\mu\text{-O})(\mu\text{-RCO}_2)(N\text{-MeIm})_8](ClO_4)_3$ (where R = H (**4**), CH_3 (**6**), or C_6H_5 (**7**)); addition of the respective carboxylate ligand in stoichiometric amount to a solution of **3** in *N*-MeIm affords these complexes in high yields. Attempts to add a third bridge to complexes **4**, **6**, and **7** to form the (μ-oxo)bis(μ-carboxylato)diiron(III) species result in the isolation of the previously known triiron(III) μ-η^3-oxo clusters $[\{Fe(\mu\text{-RCO}_2)_2(N\text{-MeIm})\}_3O](ClO_4)$ (**8**). The structures of **3**, **4**, **6**, and **7** allow one, for the first time, to inspect the various features of the $\{Fe_2(\mu\text{-O})(\mu\text{-RCO}_2)\}^{3+}$ moiety with no strain from the ligand framework.

Introduction

There has been a tremendous effort in the past two decades to model the active sites of enzymes that contain non-heme diiron cores.[1−5] In such pursuit, attempts have been directed toward preparation of small molecules that have either some structural similarity to the enzyme or reactivity that is reminiscent of the native enzyme to some extent. The crystallographic structures of the enzymes reveal relatively conserved coordination of histidine and mono- or bis-aspartate (and/or glutamate) ligands bridging a μ-oxo diiron center.[1,2,5−7] Syntheses of simple model complexes with a discrete (μ-oxo)mono- or bis(μ-carboxylato)diiron(III) core are often beset with problems due to the propensity of iron(III) salts in basic medium to form large extended structures bridged by carboxylate and oxo or hydroxo groups.[2,3,8] Two common strategies used to overcome the thermodynamic tendency of Fe^{3+} to form clusters are as follows.[2,4] The first one involves the use of multidentate nitrogen ligands designed to block off the peripheral coordination sites of the (μ-oxo)(μ-carboxylato)diiron cores. This prevents further bridging and cluster formation.[2−4,9,10] In some cases, multidentate amine ligands have been designed as a single unit with a large enough cavity to bring the two iron atoms within bridging distance.[2−4] The second strategy involves the use of specifically designed carboxylate ligands which prevent the formation of large iron−oxo

---

* To whom correspondence should be addressed. E-mail: mascharak@chemistry.ucsc.edu.

[†] University of California, Santa Cruz.

[‡] University of California, Davis.

(1) Feig, A. L.; Lippard, S. J. *Chem. Rev.* **1994**, *94*, 759.

(2) Du Bois, J.; Mizoguchi, T. J.; Lippard, S. J. *Coord. Chem. Rev.* **2000**, *200−202*, 443.

(3) Kurtz, D. M., Jr. *Chem. Rev.* **1990**, *90*, 585.

(4) Marlin, D. S.; Mascharak, P. K. In *Encyclopedia of Catalysis: Biomimetic Catalysis by Models of Non-Heme Iron Enzymes*; Horváth, I. T., Ed.; John Wiley & Sons: New York, in press.

(5) Solomon, E. I.; Brunold, T. C.; Davis, M. I.; Kemsley, J. N.; Lee, S.-K.; Lehnert, N.; Neese, F.; Skulan, A. J.; Yang, Y.-S.; Zhou, J. *Chem. Rev.* **2000**, *100*, 235.

(6) Wallar, B. J.; Lipscomb, J. D. *Chem. Rev.* **1996**, *96*, 2625.

(7) Que, L. Jr.; True, A. E. In *Progress in Inorganic Chemistry Bioinorganic Chemistry*; Lippard, S. J., Ed.; John Wiley & Sons: New York, 1990; Vol. 38, p 97.

(8) Lippard, S. J. *Angew. Chem., Int. Ed. Engl.* **1988**, *27*, 344.

10.1021/ic0206140 CCC: $25.00

clusters via steric hindrance or via selective positioning of the carboxylate groups on an organic platform.[2] To our knowledge, simple (μ-oxo)(μ-carboxylato)diiron(III) cores made up of untethered monodentate amine and simple bridging carboxylate ligands have not been synthesized and structurally characterized so far.

We have been interested in the assembly of discrete (μ-oxo)mono- and bis-(μ-carboxylato)diiron(III) cores from *N*-methylimidazole (*N*-MeIm) and simple carboxylate donors such as formate, acetate, and benzoate. Here, we report several such complexes derived from a simple monomeric iron(III) precursor, [Fe(*N*-MeIm)$_6$](ClO$_4$)$_3$ (**1**). In our systematic approach, we have isolated and structurally characterized the (μ-oxo)diiron(III) complex, [Fe$_2$(μ-O)(*N*-MeIm)$_{10}$](ClO$_4$)$_4$ (**3**). When a solution of **3** in neat *N*-MeIm is exposed to a stoichiometric amount of CO$_2$, the (μ-oxo)mono(μ-carboxylato)diiron(III) species [Fe$_2$(μ-O)(μ-HCO$_2$)(*N*-MeIm)$_8$](ClO$_4$)$_3$ (**4**) is obtained in moderate yield. If an excess of CO$_2$ is used, this reaction leads to the rapid formation of the methyl carbonate complex [Fe$_2$(μ-O)(μ-CH$_3$OCO$_2$)(*N*-MeIm)$_8$](ClO$_4$)$_3$ (**5**). Complex **3** may also be directly converted to [Fe$_2$(μ-O)(μ-RCO$_2$)(*N*-MeIm)$_8$](ClO$_4$)$_3$ (where R = H (**4**), CH$_3$ (**6**), or C$_6$H$_5$ (**7**)) upon addition of the respective carboxylate ligand in a stoichiometric amount. Interestingly, when additional carboxylates are added to form the corresponding (μ-oxo)bis(μ-carboxylato)diiron(III) species, only the well-known triiron(III) μ-η^3-oxo clusters [{Fe(μ-RCO$_2$)$_2$(*N*-MeIm)}$_3$O](ClO$_4$) (**8**)[11,12] were obtained. Our results indicate that although the (μ-oxo)mono(μ-carboxylato)diiron(III) core with monodentate ligand *N*-MeIm is thermodynamically stable and even forms upon CO$_2$ fixation, the corresponding (μ-oxo)bis(μ-carboxylato)diiron(III) species is not as robust and is readily converted to the very stable cluster **8**.

Experimental Section

[Fe(DMF)$_6$](ClO$_4$)$_3$ was synthesized by following the published procedure.[13] *N*-Methylimidazole (Aldrich Chem. Co.) was distilled from sodium metal before use. All solvents were purified and/or dried by standard techniques and distilled prior to use.

***Synthesis Safety Note*.** Perchlorate salts should be handled with caution. Although no explosion was encountered in this work, metal perchlorates could detonate upon heating.

Synthesis of Compounds. [Fe(*N*-MeIm)$_6$](ClO$_4$)$_3$ (1). A batch of [Fe(DMF)$_6$](ClO$_4$)$_3$ (20 g, 25.6 mmol) was added to *N*-MeIm (20 mL), and the resultant red solution was allowed to stir for 1 h. Excess *N*-MeIm and the DMF were then distilled off under vacuum, and dry CH$_3$CN (30 mL) was added to the remaining residue. The resultant orange precipitate was filtered off and dried under vacuum (19 g, 90%). Complex **1** was recrystallized as large red needles from THF/*N*-MeIm (2:1 v/v). Selected IR frequencies (KBr disk, cm^{-1}): 3153 (m), 3129 (m), 1546 (m), 1519 (m), 1420 (w), 1330 (w), 1238 (m), 1099 (s), 1027 (w), 952 (w), 845 (m), 757 (m), 655 (m), 618 (m). Anal. Found: C, 34.12; H, 4.20; N, 19.93. Calcd for C$_{24}$H$_{36}$N$_{12}$FeCl$_3$O$_{12}$: C, 34.04; H, 4.29; N, 19.85.

[Fe$_2$(μ-O)(*N*-MeIm)$_{10}$](ClO$_4$)$_4$·2THF (3·2THF). To a solution of **1** (1.0 g, 1.2 mmol) in neat *N*-MeIm was added a small aliquot of H$_2$O (0.01 mL). After a brief stirring period (~1 h), the solution was filtered, and THF was carefully layered on the top (2:1 THF/*N*-MeIm v/v). Large red blocks of **3**·2THF, suitable for X-ray crystallography, were collected within 48 h (0.5 g, 60%). Selected IR frequencies (KBr disk, cm^{-1}): 3138 (m), 1543 (m), 1521 (m), 1419 (w), 1287 (w), 1236 (m), 1089 (s), 947 (m), 839 (m), 763 (s, Fe−O−Fe), 659 (s), 624 (s). Anal. Found: C, 38.53; H, 5.20; N, 18.57. Calcd for C$_{48}$H$_{76}$N$_{20}$Fe$_2$Cl$_4$O$_{19}$: C, 38.67; H, 5.14; N, 18.79.

[Fe$_2$(μ-O)(μ-HCO$_2$)(*N*-MeIm)$_8$](ClO$_4$)$_3$·THF (4·THF). A solution of **3** (0.1 g, 0.06 mmol) in neat *N*-MeIm (2 mL) was placed in a screwcap 5 dram vial, and a layer of THF (4 mL) was placed on the top of it. A batch of 1 mL of CO$_2$ was then introduced into the THF layer with the aid of a gas syringe, and the closed system was stored at room temperature. Green cystals of **4** were isolated after 7 days in 30% yield. Selected IR frequencies (KBr disk, cm^{-1}): 3135 (m), 1560 (w), 1540 (m), 1518 (m), 1423 (m), 1364 (w), 1288 (w), 1235 (w), 1093 (s), 946 (m), 830 (m), 763 (s, Fe−O−Fe), 658 (s), 623 (s) cm^{-1}. Anal. Found: C, 37.23; H, 4.72; N, 18.67. Calcd for C$_{37}$H$_{57}$N$_{16}$Fe$_2$Cl$_3$O$_{16}$: C, 37.03; H, 4.79; N, 18.68.

[Fe$_2$(μ-O)(μ-HCO$_2$)(*N*-MeIm)$_8$](ClO$_4$)$_3$·THF (4·THF), [Fe$_2$(μ-O)(μ-CH$_3$CO$_2$)(*N*-MeIm)$_8$](ClO$_4$)$_3$ (6·2.5THF), and [Fe$_2$(μ-O)(μ-C$_6$H$_5$CO$_2$)(*N*-MeIm)$_8$](ClO$_4$)$_3$ (7). To a solution of **3** (0.5 g, 0.3 mmol) in neat *N*-MeIm (2 mL) was added either HCO$_2$Na (0.023 g, 0.3 mmol), CH$_3$CO$_2$Na (0.029 g, 0.3 mmol) or C$_6$H$_5$CO$_2$H (0.041 g, 0.3 mmol) for **4**, **6**, or **7** respectively. The reaction mixtures were stirred for 5 h and then filtered. Each was then layered carefully with THF (4 mL), and within 2 days, large green blocks of the respective complex were isolated (**4** 0.28 g, 70%; **6** 0.36 g, 82%; **7** 0.3 g, 76%). The X-ray crystal structures of **4**·THF and **6**·2.5THF have been determined. Selected IR frequencies (KBr disk, cm^{-1}): **4**, 3135 (m), 1560 (w), 1540 (m), 1518 (m), 1423 (m), 1364 (w), 1288 (w), 1235 (w), 1093 (s), 946 (m), 830 (m), 763 (s, Fe−O−Fe), 658 (s), 623 (s) cm^{-1}; **6**, 3136 (m), 1561 (m), 1540 (m), 1519 (m), 1424 (m), 1368 (w), 1288 (w), 1235 (m), 1093 (s), 1028 (w), 947 (w), 835 (w), 835 (m), 757 (s, Fe−O−Fe), 658 (s), 623 (s). Anal. for **6**·2.5THF Found: C, 39.98; H, 5.31; N, 17.03. Calcd for C$_{44}$H$_{71}$N$_{16}$Fe$_2$Cl$_3$O$_{17.5}$: C, 39.97; H, 5.41; N, 16.95.

[Fe$_2$(μ-O)(μ-CH$_3$OCO$_2$)(*N*-MeIm)$_8$](ClO$_4$)$_3$·0.5*N*-MeIm·THF (5·0.5*N*-MeIm·THF). Excess CO$_2$ was added to a solution of **3** (0.5 g, 0.3 mmol) in neat *N*-MeIm (2 mL) when the color changed rapidly from red to green. A batch of 6 mL of THF was layered on the top of this green solution, and the mixture was stored at room temperature in an airtight vial for 7 days. Large green plates of **5** were isolated in 45% yield. Selected IR frequencies (KBr disk, cm^{-1}): 3136 (m), 1561 (w), 1540 (m), 1519 (w), 1235 (m), 1093 (s), 945 (w), 830 (m), 757 (s, Fe−O−Fe), 658 (s), 623 (s). Anal. Found: C, 38.01; H, 4.79; N, 18.57. Calcd for C$_{40}$H$_{62}$N$_{17}$Fe$_2$Cl$_3$O$_{17}$: C, 37.80; H, 4.92; N, 18.73.

X-ray Data Collection and Structure Solution and Refinement. Diffraction experiments were performed on a Bruker SMART 1000 diffractometer at 92 K (in case of **1**, **3**, **4**, and **5**) and on a Siemens P3 machine at 130 K (in case of **6**). The structures were solved by the use of SHELXS-97 package, and the data were corrected for absorption effects. The refinement of the structure of **5** was less satisfactory due to difficulties in modeling the disordered THF and *N*-MeIm molecules in the crystal lattice. Machine parameters, crystal data, and data collection parameters are sum-

---

[9] Ookubo, T.; Sugimoto, H.; Nagayama, T.; Masuda, H.; Sato, T.; Tanaka, K.; Maeda, Y.; Okawa, H.; Hayashi, Y.; Uehara, A.; Suzuki, M. *J. Am. Chem. Soc.* **1996**, *118*, 701.

[10] Dong, Y.; Yan, S.; Young, V. G., Jr.; Que, L., Jr. *Angew. Chem., Int. Ed. Engl.* **1996**, *35*, 618.

[11] Oh, S. M.; Hendrickson, D. N.; Hassett, K. L.; Davis, R. E. *J. Am. Chem. Soc.* **1985**, *107*, 8009.

[12] Wu, F.-J.; Kurtz, D. M., Jr. *J. Am. Chem. Soc.* **1989**, *111*, 6563.

[13] Hodgkinson, J.; Jordan, R. B. *J. Am. Chem. Soc.* **1973**, *95*, 763.

Table 1. Summary of Crystal Data and Intensity Collection and Structure Refinement Parameters for [Fe(*N*-MeIm)$_6$](ClO$_4$)$_3$ (**1**), [Fe$_2$(*μ*-O)(*N*-MeIm)$_{10}$](ClO$_4$)$_4$·2THF (**3**·2THF), [Fe$_2$(*μ*-O)(*μ*-HCO$_2$)(*N*-MeIm)$_8$](ClO$_4$)$_3$·THF (**4**·THF), [Fe$_2$(*μ*-O)(*μ*-CH$_3$OCO$_2$)(*N*-MeIm)$_8$](ClO$_4$)$_3$·0.5*N*-MeIm·THF (**5**·0.5*N*-MeIm·THF), and [Fe$_2$(*μ*-O)(*μ*-CH$_3$CO$_2$)(*N*-MeIm)$_8$](ClO$_4$)$_3$·2.5THF (**6**·2.5THF)

	1	**3**·2THF	**4**·THF	**5**·0.5*N*-MeIm·THF	**6**·2.5THF
empirical formula	$C_{24}H_{36}N_{12}FeCl_3O_{12}$	$C_{48}H_{76}N_{20}Fe_2Cl_4O_{19}$	$C_{37}H_{57}N_{16}Fe_2Cl_3O_{16}$	$C_{40}H_{62}N_{17}Fe_2Cl_3O_{17}$	$C_{44}H_{71}N_{16}Fe_2Cl_3O_{17.5}$
fw	846.85	1490.79	1200.04	1271.12	1322.22
cryst color, habit	red needle	red plate	green plate	green needle	green plate
T, K	92(2)	92(2)	92(2)	92(2)	130(2)
cryst syst	trigonal	monoclinic	monoclinic	triclinic	triclinic
space group	$R\bar{3}c$	$P2_1/c$	$C2/c$	$P\bar{1}$	$P\bar{1}$
a, Å	19.511(3)	13.5262(14)	27.106(4)	13.0447(9)	12.363(3)
b, Å	19.511(3)	17.0491(15)	10.1860(10)	13.5509(9)	14.151(4)
c, Å	15.354(3)	28.578(3)	20.362(3)	18.4953(14)	19.276(4)
α, deg	90	90	90	89.336(4)	103.499(18)
β, deg	90	90.060(2)	96.247(7)	82.316(4)	99.757(18)
γ, deg	120	90	90	77.390(4)	109.673(18)
V, Å^3	5061.9(15)	6590.4(11)	5588.6(13)	3161.3(4)	2972.3(12)
Z	6	4	4	2	2
d(calcd), g cm^{-3}	1.667	1.503	1.426	1.335	1.477
abs coeff, mm^{-1}	0.764	0.686	0.738	0.658	0.703
GOF[a] on F^2	0.961	1.015	1.055	1.198	1.021
R1,[b] %	3.93	6.65	8.04	9.85	7.06
wR2,[c] %	6.92	17.52	22.10	28.86	17.71

[a] GOF = $[\Sigma[w(F_o^2 - F_c^2)^2]/(M - N)]^{1/2}$ (M = number of reflections, N = number of parameters refined). [b] R1 = $\Sigma||F_o| - |F_c||/\Sigma|F_o|$. [c] wR2 = $[\Sigma[w(F_o^2 - F_c^2)^2]/\Sigma[w(F_o^2)^2]]^{1/2}$.

Scheme 1 [a]

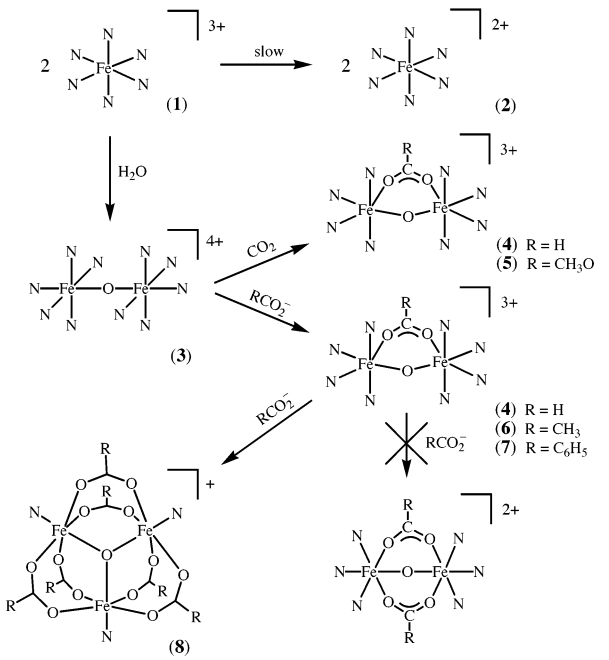

[a] N denotes ligated *N*-MeIm.

marized in Table 1 while selected bond distances and angles are listed in Table 2.

Results and Discussion

Monomeric [Fe(*N*-MeIm)$_6$](ClO$_4$)$_3$ (**1**) was prepared by dissolving anhydrous [Fe(DMF)$_6$](ClO$_4$)$_3$ in freshly distilled neat *N*-MeIm. Although very stable in the solid state, **1** is relatively unstable in solution and is slowly reduced to the more stable Fe^{II} species [Fe(*N*-MeIm)$_6$](ClO$_4$)$_2$ (**2**) (Scheme 1).[14] This behavior is in line with the general instability of iron(III) complexes with monodentate nitrogen ligands.[15] Use of *N*-MeIm as the solvent is the key for the successful isolation of **1** in the present work. A previous iron(III) complex of *N*-MeIm, namely *trans*-[Fe(*N*-MeIm)$_4$F$_2$]BF$_4$, has also been isolated in [*N*-MeImH][BF$_4$], an ionic liquid medium.[16] Under a dinitrogen atmosphere, monomer **1** is converted to the *μ*-oxo species [Fe$_2$(*μ*-O)(*N*-MeIm)$_{10}$](ClO$_4$)$_4$ (**3**) upon addition of 0.5 equiv of H$_2$O (per iron) in neat *N*-MeIm. Large red plates of **3**·2THF deposited within 48 h from THF/*N*-MeIm (2:1 v/v) solutions. Complex **3** is a convenient starting synthon for (*μ*-oxo)mono(*μ*-carboxylato)diiron(III) complexes. Addition of stoichiometric amounts of various carboxylates (RCO$_2^-$, R = H, CH$_3$, C$_6$H$_5$) to solution of **3** readily affords the (*μ*-oxo)mono(*μ*-carboxylato)diiron(III) complexes **4**, **6**, and **7** in high yields (Scheme 1). However, it is interesting to note that this reactivity of **3** cannot be utilized to synthesize the (*μ*-oxo)bis(*μ*-carboxylato)diiron(III) complexes with *N*-MeIm as the terminal ligand. Attempts to add a second *μ*-carboxylato bridge to these complexes and form the (*μ*-oxo)bis(*μ*-carboxylato)diiron(III) species have resulted only in isolation of the respective triiron cluster[17] well-known in iron(III) chemistry (Scheme 1). [3,8,18]

Complex **3** exhibits an unusual reactivity toward CO$_2$. If a small amount of CO$_2$ (no more than 1 equiv) is carefully added to the THF layer during crystallization of **3** from *N*-MeIm solution, large green crystals of the formato-bridged complex [Fe$_2$(*μ*-O)(*μ*-HCO$_2$)(*N*-MeIm)$_8$](ClO$_4$)$_3$·THF (**4**·THF) form in the reaction vial (Scheme 1).[19] Formation of

---

(14) Miller, L. L.; Jacobson, R. A.; Chen, Y.-S.; Kurtz, D. M., Jr. *Acta Crystallogr*. **1989**, *C45*, 527.

(15) Cotton, F. A.; Wilkinson, G. *Advanced Inorganic chemistry*, 5th ed.; Wiley-Interscience: New York, 1988; p 718.

(16) Christie, S.; Subramanian, S.; Wang, L.; Zaworotko, M. J. *Inorg. Chem.* **1993**, *32*, 5415.

(17) Spectroscopic parameters of [{Fe(*μ*-C$_6$H$_5$CO$_2$)$_2$(*N*-MeIm)}$_3$O](ClO$_4$) (**8**, R = C$_6$H$_5$) were compared with those of an authentic sample.[12] The crystal parameters and overall features of the structure of the cation of **8**·CH$_2$Cl$_2$ match those of [{Fe(*μ*-C$_6$H$_5$CO$_2$)$_2$(py)}$_3$O](NO$_3$)·CH$_2$Cl$_2$. [18]

(18) Bond, A. M.; Clark, R. J. H.; Humphrey, D. G.; Panayiotopoulos, P.; Skelton, B. W.; White, A. H. *J. Chem. Soc., Dalton Trans*. **1998**, *11*, 1845.

Table 2. Selected Bond Distances (Å) and Angles (deg)

Complex **1**			
Fe(1)−N(1)	2.1133(15)	Fe(1)−N(1A−1D)	2.1134(15)
N(1)−C(1)	1.386(2)	N(1)−C(3)	1.331(2)
N(2)−C(3)	1.341(2)	Cl(1)−O(1)	1.4369(15)
N(1)−Fe(1)−N(1A)	180.00(6)	N(1A)−Fe(1)−N(1B)	89.04(6)
Complex **3**			
Fe(1)−N(1)	2.292(3)	Fe(1)−O(1)	1.811(3)
Fe(1)−N(3)	2.153(3)	Fe(1)−N(5)	2.131(3)
Fe(1)−N(7)	2.173(3)	Fe(1)−N(9)	2.123(3)
Fe(2)−O(1)	1.818(3)	Fe(2)−N(11)	2.282(3)
Fe(2)−N(13)	2.165(3)	Fe(2)−N(17)	2.168(3)
Fe(2)−N(19)	2.125(3)	Cl(1)−O(3)	1.438(4)
Fe(1)−O(1)−Fe(2)	169.34(17)	O(1)−Fe(1)−N(3)	95.72(12)
N(1)−Fe(1)−O(1)	178.12(13)	N(3)−Fe(1)−N(7)	168.29(13)
N(5)−Fe(1)−N(9)	168.85(13)	O(1)−Fe(2)−N(11)	177.97(12)
N(13)−Fe(2)−N(17)	165.28(12)	N(15)−Fe(2)−N(19)	169.55(13)
N(5)−Fe(1)−N(3)	87.52(14)	N(15)−Fe(2)−N(13)	89.15(13)
Complex **4**			
Fe(1)−N(1)	2.250(4)	Fe(1)−N(3)	2.129(5)
Fe(1)−N(5)	2.146(5)	Fe(1)−N(7)	2.137(4)
Fe(1)−O(1)	1.8030(19)	Fe(1)−O(2)	2.059(3)
Fe(1A)−O(1)	1.8030(18)	C(17)−O(2)	1.246(5)
Fe(1)−O(1)−Fe(1A)	131.3(2)	N(1)−Fe(1)−O(1)	178.87(15)
N(7)−Fe(1)−O(2)	164.79(15)	N(3)−Fe(1)−N(5)	172.16(17)
O(1)−Fe(1)−O(2)	99.65(16)	Fe(1)−O(2)−C(17)	130.2(4)
O(1)−Fe(1)−N(7)	95.46(16)	N(3)−Fe(1)−N(7)	92.39(16)
Complex **5**			
Fe(1)−N(1)	2.224(6)	Fe(1)−N(3)	2.155(5)
Fe(1)−N(5)	2.139(5)	Fe(1)−N(7)	2.155(6)
Fe(1)−O(1)	1.804(4)	Fe(1)−O(2)	2.026(4)
C(33)−O(2)	1.282(8)	C(33)−O(3)	1.265(8)
C(33)−O(4)	1.344(9)	C(34)−O(4)	1.443(10)
Fe(1)−O(1)−Fe(2)	131.7(2)	O(1)−Fe(1)−O(2)	99.89(18)
O(2)−C(33)−O(3)	126.7(6)	O(2)−C(33)−O(4)	115.3(7)
O(1)−Fe(1)−N(3)	91.13(19)	O(2)−Fe(1)−N(3)	168.6(2)
N(1)−Fe(1)−O(1)	173.86(18)	O(3)−Fe(2)−N(11)	168.50(18)
O(3)−Fe(2)−N(15)	89.4(2)	C(33)−O(4)−C(34)	121.2(7)
Complex **6**			
Fe(1)−N(1)	2.149(4)	Fe(1)−N(3)	2.236(3)
Fe(1)−O(1)	1.795(3)	Fe(2)−O(1)	1.797(3)
Fe(1)−O(2)	2.057(3)	Fe(2)−O(3)	2.047(3)
O(3)−C(33)	1.250(5)	O(2)−C(33)	1.251(5)
Fe(2)−N(17)	2.233(3)	Fe(2)−N(7)	2.134(4)
Fe(2)−N(9)	2.121(3)	C(33)−C(34)	1.498(6)
Fe(1)−O(1)−Fe(2)	133.09(16)	O(1)−Fe(1)−O(2)	97.96(12)
O(1)−Fe(1)−N(3)	175.85(13)	O(1)−Fe(2)−N(17)	178.56(13)
N(1)−Fe(1)−N(13)	174.94(13)	Fe(1)−O(2)−C(33)	131.6(3)
O(2)−C(33)−O(3)	125.7(4)	O(1)−Fe(2)−O(3)	98.43(12)
O(1)−Fe(1)−N(1)	93.66(13)	O(2)−C(33)−C(34)	118.3(4)

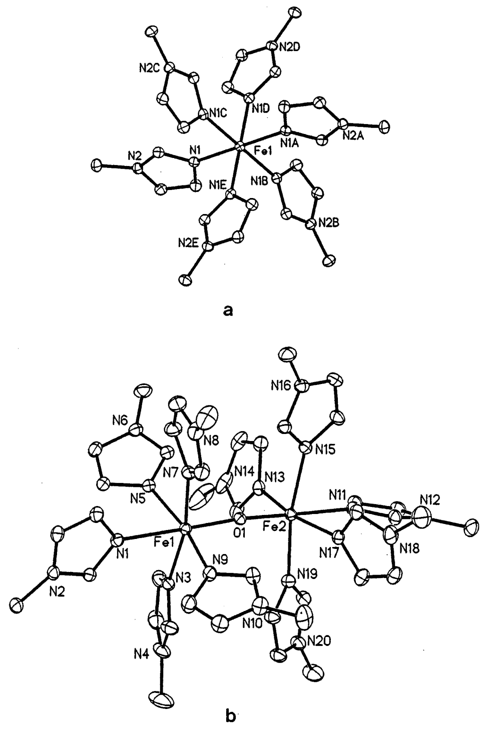

Figure 1. Thermal ellipsoid (probability level 50%) plot of (a) of $[Fe(N\text{-}MeIm)_6]^{3+}$ (cation of **1**) and (b) $[Fe_2(\mu\text{-}O)(N\text{-}MeIm)_{10}]^{4+}$ (cation of **3**) with the atom-labeling scheme. H atoms are omitted for the sake of clarity.

formato bridge in the diiron(III) core via reaction of CO_2 has not been observed before. The presence of excess *N*-MeIm is a requirement for this reactivity; **4** is not obtained when a solution of **3** in MeCN or DMF is exposed to CO_2. When excess CO_2 is added to **3** in *N*-MeIm solution, the color rapidly changes from red to emerald green. Large green plates of the methyl carbonate complex $[Fe_2(\mu\text{-}O)(\mu\text{-}CH_3OCO_2)(N\text{-}MeIm)_8](ClO_4)_3$ (**5**) are isolated within 1 week upon addition of THF to this solution (Scheme 1). These reactions have been discussed in detail in a separate section (vide infra). Complexes **4**, **6**, and **7** are stable in anhydrous acetonitrile for several days. However, in the presence of excess *N*-MeIm, they eventually decompose to other products including **2**.

Structure of $[Fe(N\text{-}MeIm)_6](ClO_4)_3$ (1) and $[Fe_2(\mu\text{-}O)(N\text{-}MeIm)_{10}](ClO_4)_4$ (3). The structures of $[Fe(N\text{-}MeIm)_6]^{3+}$ (the cation of **1**) and $[Fe_2(\mu\text{-}O)(N\text{-}MeIm)_{10}]^{4+}$ (the cation of **3**) are shown in Figure 1. The geometry around iron in **1** is octahedral, and the Fe(III)−N bond is 2.1134(15) Å long. This bond distance is similar to the Fe(III)−N distance in $[Fe(N\text{-}MeIm)_4F_2]BF_4$[16] but shorter than the Fe(II)−N bond distance (2.207(10) Å) observed in $[Fe(N\text{-}MeIm)_6]^{2+}$.[14] The Fe(III)−N distances of **3** are, however, slightly longer than that in **1** (Table 2). In particular, Fe(III)−N bonds trans to the bridging oxygen are noticeably long (average 2.287(3) Å). The Fe(III)−O distance (average 1.815(3) Å) and the Fe−O−Fe angle (169.34(17)°) are both within the range of simple μ-oxodiiron(III) complexes.[20]

Structure of $[Fe_2(\mu\text{-}O)(\mu\text{-}HCO_2)(N\text{-}MeIm)_8](ClO_4)_3$ (4). To date, a few complexes with monocarboxylato-bridged diiron(III) unit have been reported.[21−25] These reported

---

(19) In the syntheses of **4** and **5**, a small amount of **2** was also isolated from the reaction mixture. The almost colorless crystals accumulate near the junction of the two solutions. These crystals can be physically separated from the desired product without much trouble.

(20) Dorfman, J. R.; Girerd, J.-J.; Simhon, E. D.; Stack, T. D. P.; Holm, R. H. *Inorg. Chem.* **1984**, *23*, 4407 and references therein.

(21) Yan, S.; Que, L., Jr.; Taylor, L. F.; Anderson, O. P. *J. Am. Chem. Soc.* **1988**, *110*, 5222.

(22) Yan, S.; Cox, D. D.; Pearce, L. L.; Juarez-Garcia, C.; Que, L., Jr.; Zhang, J. H.; O'Connor, C. J. *Inorg. Chem.* **1989**, *28*, 2509.

(23) Norman, R. E.; Yan, S.; Que, L., Jr.; Backes, G.; Ling, J.; Sanders-Loehr, J.; Zhang, J. H.; O'Connor, C. J. *J. Am. Chem. Soc.* **1990**, *112*, 1554.

(24) Norman, R. E.; Leising, R. A.; Yan, S.; Que, L., Jr. *Inorg. Chim. Acta* **1998**, *273*, 393.

(25) Lee, D.; Lippard, S. J. *Inorg. Chem.* **2002**, *41*, 827 and references therein.

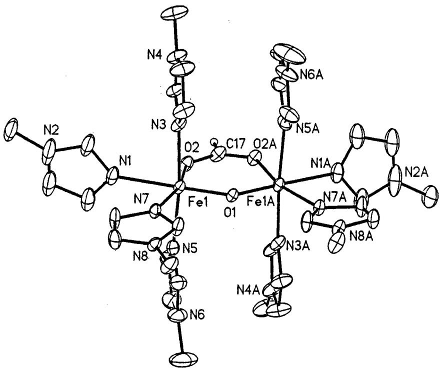

Figure 2. Thermal ellipsoid (probability level 50%) plot of $[Fe_2(\mu\text{-O})(\mu\text{-HCO}_2)(N\text{-MeIm})_8]^{3+}$ (cation of **4**) with the atom-labeling scheme. H atoms are omitted for the sake of clarity.

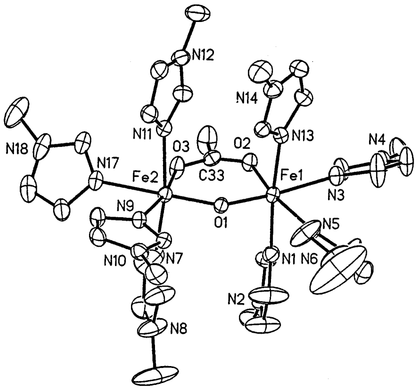

Figure 3. Thermal ellipsoid (probability level 50%) plot of $[Fe_2(\mu\text{-O})(\mu\text{-CH}_3CO_2)(N\text{-MeIm})_8]^{3+}$ (cation of **6**) with the atom-labeling scheme. H atoms are omitted for the sake of clarity.

complexes are all derived from multidentate ligands. The structure of $[Fe_2(\mu\text{-O})(\mu\text{-HCO}_2)(N\text{-MeIm})_8]^{3+}$ (shown in Figure 2) allows one, for the first time, to inspect the various features of the $\{Fe_2(\mu\text{-O})(\mu\text{-HCO}_2)\}^{3+}$ moiety under no strain imposed by the ligand framework. For example, the Fe−O−Fe angle of **4** (131.3(2)°) is larger than that of $[Fe_2(\mu\text{-O})(\mu\text{-HCO}_2)(TPA)_8](ClO_4)_3$ (TPA = the tetradentate tripodal ligand tris(2-pyridylmethyl)amine), 128.6(3)°).[24] Consequently, the Fe−Fe distance of **4** (3.285(5) Å) is slightly longer than that of $[Fe_2(\mu\text{-O})(\mu\text{-HCO}_2)(TPA)_8](ClO_4)_3$ (3.231(5) Å). Comparison of the bridging portion of **3** and **4** indicates that the formation of one carboxylato bridge causes reduction of the Fe−O−Fe angle (from 169.34(17)° in **3** to 131.3(2)° in **4**) and slight shortening of the Fe−O distance (from 1.815(3) Å in **3** to 1.8030(19) Å in **4**). The Fe(III)−N bond distances of **4** (average 2.165(5) Å) are, however, very similar to those in **3** (average 2.174(4) Å). The Fe(III)−O_{carb} (carboxylato O) distance in **4** (2.059(3) Å) is close to that observed in other complexes with the $\{Fe_2(\mu\text{-O})(\mu\text{-RCO}_2)\}^{3+}$ moiety.[21−25]

Structure of $[Fe_2(\mu\text{-O})(\mu\text{-CH}_3CO_2)(N\text{-MeIm})_8](ClO_4)_3$ (6). The structure of the cation of the mono-μ-acetato μ-oxodiiron(III) complex **6**, namely $[Fe_2(\mu\text{-O})(\mu\text{-CH}_3CO_2)(N\text{-MeIm})_8]^{3+}$, is shown in Figure 3. Except for a slightly larger Fe−O−Fe angle (133.09(16)°), the structure is very similar to that of **4**. Compared to the structure of $[Fe_2(\mu\text{-O})(\mu\text{-CH}_3CO_2)(TPA)_2]^{3+}$, the other mono-μ-acetato complex,[22] the structure of $[Fe_2(\mu\text{-O})(\mu\text{-CH}_3CO_2)(N\text{-MeIm})_8]^3$ is more symmetric. For example, while $[Fe_2(\mu\text{-O})(\mu\text{-CH}_3CO_2)(TPA)_2]^{3+}$ exhibits two distinctly diffrent Fe(III)−O_{carb} distances (1.972(6) and 2.038(6) Å), $[Fe_2(\mu\text{-O})(\mu\text{-CH}_3CO_2)(N\text{-MeIm})_8]^{3+}$ comprises very similar Fe(III)−O_{carb} distances (2.057(3) and 2.047(3) Å).

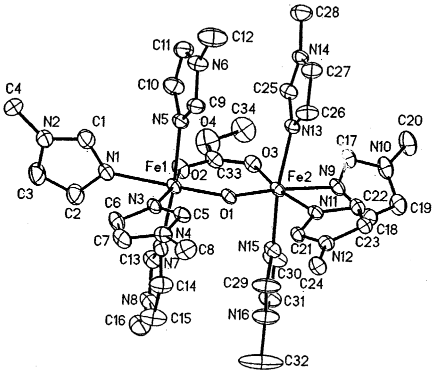

Figure 4. Thermal ellipsoid (probability level 50%) plot of $[Fe_2(\mu\text{-O})(\mu\text{-CH}_3OCO_2)(N\text{-MeIm})_8]^{3+}$ (the cation of **5**) with the atom-labeling scheme. H atoms are omitted for the sake of clarity.

Several di-μ-acetato μ-oxodiiron(III) complexes have been synthesized as models for diiron proteins such as hemerethrin.[1,26−28] It is quite interesting to note changes in the diiron(III) core when the second bridging acetate is introduced. The most noticeable change occurs in the Fe−O−Fe angle although the Fe−O distance remains more or less unchanged. For example, the Fe−O−Fe angles in $[Fe_2(\mu\text{-O})(\mu\text{-CH}_3CO_2)_2(HB(pz)_3)_2]^{26}$ and $[Fe_2(\mu\text{-O})(\mu\text{-CH}_3CO_2)_2Cl_2(bpy)_2]^{28}$ are 123.6(1)° and 123.9(2)°, respectively, (much smaller than **6**) while the Fe−O distance in both complexes is ∼1.78 Å, a value almost identical to that observed in **4** and **6**. The Fe−O−Fe angle is even smaller in $[Fe_2(\mu\text{-O})(\mu\text{-CH}_3CO_2)_2(Me_3TACN)_2]^{2+}$ (119.7(1) Å).[25] Overall, the second acetate bridge shortens the Fe−Fe distance. Thus, while the mono-μ-acetato μ-oxodiiron(III) complexes **6** and $[Fe_2(\mu\text{-O})(\mu\text{-CH}_3CO_2)(TPA)_2](ClO_4)_3$ exhibit an Fe−Fe distance of 3.29 and 3.24 Å, respectively, the di-μ-acetato μ-oxodiiron(III) complexes $[Fe_2(\mu\text{-O})(\mu\text{-CH}_3CO_2)_2(HB(pz)_3)_2]$, $[Fe_2(\mu\text{-O})(\mu\text{-CH}_3CO_2)_2Cl_2(bpy)_2]$, and $[Fe_2(\mu\text{-O})(\mu\text{-CH}_3CO_2)_2(Me_3TACN)_2](ClO_4)_2$ have their Fe−Fe distances in the close range 3.12−3.15 Å.

Structure of $[Fe_2(\mu\text{-O})(\mu\text{-CH}_3OCO_2)(N\text{-MeIm})_8](ClO_4)_3$ (5). The structure of the μ-oxodiiron(III) complex with bridging methyl carbonate, namely $[Fe_2(\mu\text{-O})(\mu\text{-CH}_3OCO_2)(N\text{-MeIm})_8]^{3+}$ (the cation of **5**), is shown in Figure 4. Although a large number of carbonato complexes (including bridging carbonate) are reported,[29] examples of iron complexes with bound carbonate have been limited.[30−34] The rapid formation of oxo- and hydroxo-bridged polymeric species by iron salts in aqueous (or mixed) medium in the

---

(26) Armstrong, W. H.; Spool, A.; Papaefthymiou, G. C.; Frankel, R. B.; Lippard, S. J. *J. Am. Chem. Soc.* **1984**, *106*, 3653.

(27) Hartman, J. A. R.; Rardin, R. L.; Chaudhuri, P.; Pohl, K.; Wieghardt, K.; Nuber, B.; Weiss, J.; Papaefthymiou, G. C.; Frankel, R. B.; Lippard, S. J. *J. Am. Chem. Soc.* **1987**, *109*, 7387.

(28) Vincent, J. B.; Huffman, J. C.; Christou, G.; Li, Q.; Nanny, M. A.; Hendrickson, D. N.; Fong, R. H.; Fish, R. H. *J. Am. Chem. Soc.* **1988**, *110*, 6898.

(29) Palmer, D. A.; Van Eldik, R. *Chem. Rev.* **1983**, *83*, 651.

presence of carbonate or bicarbonate is responsible for this scarcity. No iron complex with bound methyl carbonate has been reported so far. The structure of **5** is unique in this regard. Comparison of the structural parameters reveals that both the Fe−O−Fe angle (131.7(2)°) and the Fe−O distance (1.804(4) Å) of **5** are very similar to those of **4** and **6**. Also, the Fe−$O_{carbonate}$ distances (2.026(4) and 2.021(5) Å) resemble the Fe−O_{carb} distances of **6** (2.057(3) and 2.047(3) Å). The metric parameters of the bound methyl carbonate are intriguing. In simple carbonate salts, the average C−O bond length is 1.285(21) Å, and the average O−C−O angle is ∼120°.[29] The two iron-bound C−O distances (C(33)−O(2) and C(33)−O(3)) of **5** are noticeably shorter than the third C−O distance (C(33)−O(4), Table 2). In addition, the O(2)−C(33)−O(3) angle is 126.7(6)°. In short, the trigonal symmetry of the carbonate is totally lost in **5**. The absence of a second diiron(III) complex with bound methyl carbonate prevents further comparison of this moiety in similar metal complexes.

Reactions with CO_2. The unexpected CO_2 fixation capability of **3** in *N*-MeIm is quite interesting and warrants further discussion. Carbon dioxide insertion into a metal−amine bond has been reported for a number of low-valent organometallic[35] and metal−amine complexes.[36] It is often believed that, in these reactions, CO_2 does not formally insert into the metal−nitrogen bond. Instead, it reacts with amines to form carbamates in solution, and a ligand exchange process affords the final metal−carbamate complexes. Formation of formato complexes via insertion of CO_2 into metal−hydrogen bonds (including Fe−H bonds) in low-valent organometallic complexes has also been reported.[29] The low-valent metal centers are presumably the source of the two electrons required for conversion of CO_2 to HCO_2^- in these reactions. In the present reactions, **1** is found to be slowly reduced to **2** in neat (and dry) *N*-MeIm solution. In DMF, a quasireversible cyclic voltammogram is recorded for **1** with $E_{1/2}$ of +0.44 V (versus saturated calomel electrode) for the Fe(III)/Fe(II) couple. The $E_{1/2}$ value indicates that *N*-MeIm stabilizes the +2 oxidation state of iron to a great extent. This explains the slow conversion of **1** into **2** in neat *N*-MeIm.[37] The source of electrons for this reduction as well as for the formation of **4** (from **3** via CO_2 fixation) has not been definitively established at this time. Oxidation of *N*-MeIm to a *N*-methylimidazolium cation could provide these electrons (Scheme 2) since electron transfer to organic cation ionic liquids has been observed in selected cases including *N*-methylimidazole.[16,38] Further proof for this comes from the fact that this reaction does not take place in pyridine. The presence of trace amount of water in the reaction mixture is most possibly the source of protons for the formation of **4** from **3**. In essence, the formate ion is formed via reaction of CO_2 and water in the presence of **3** in *N*-MeIm. Que and co-workers have reported slow formation of $[Fe_2(\mu\text{-}O)(\mu\text{-}HCO_2)(TPA)_8](ClO_4)_3$ in methanolic solution via oxidation of solvent.[24] In the present case, *N*-MeIm was distilled from metallic sodium. We therefore rule out the possibility of methanol impurity in *N*-MeIm as the source of formate.

Scheme 2 [a]

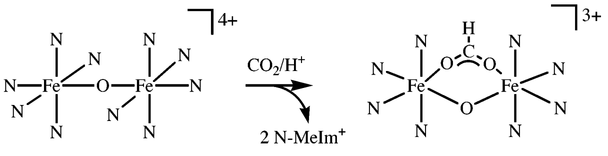

(**3**) (**4**)

[a] N denotes ligated *N*-MeIm.

When **3** is allowed to react with excess CO_2, the presence of carbonate in the reaction mixture is apparent in the formation of the methyl carbonate complex **5**. The methyl group on the $CH_3OCO_2^-$ bridge in **5** is most possibly derived from a methyl transfer reaction from the *N*-MeIm solvent.[39,40] Formation of a methyl carbonate bridge in a dinuclear hydroxo-bridged dinickel(II) macrocyclic complex upon reaction with CO_2 in methanol has recently been reported.[41] In the present case, a similar mechanism can give rise to a *μ*-bicarbonato diiron(III) intermediate which in turn can react with *N*-MeIm[42] to afford the final methyl carbonate complex **5**.[43] Although metal complexes with ligated methyl carbonate are formed upon uptake of CO_2 in basic methanolic solutions,[44,45] the absence of methanol in the present case makes such a mechanism highly unlikely. Finally, we like to emphasize that complexes **1** and **3** are the only products in *N*-MeIm (and small amount of water in case of **3**) when the synthesis is performed under an atmosphere of dinitrogen; only upon addition of appropriate amounts of CO_2 are complexes **4** and **5** isolated. It is therefore clear that the bridging groups (HCO_2^- and $CH_3OCO_2^-$) are derived from CO_2 in these reactions.

---

(30) Drüeke, S.; Wieghardt, K.; Nuber, B.; Weiss, J. *Inorg. Chem.* **1989**, *28*, 1414.
(31) Norman, R. E.; Holz, R. C.; Ménage, S.; O'Connor, C. J.; Zhang, J. H.; Que, L., Jr. *Inorg. Chem.* **1990**, *29*, 4629.
(32) Fujita, T.; Ohba, S.; Nishida, Y.; Goto, A.; Tokii, T. *Acta Crystallogr.* **1994**, *C50*, 544.
(33) Arulsamy, N.; Goodson, P. A.; Hodgson, D. J.; Glerup, J.; Michelsen, K. *Inorg. Chim. Acta* **1994**, *216*, 21.
(34) Hazell, R.; Jensen, K. B.; McKenzie, C. J.; Toftlund, H. *J. Chem. Soc., Dalton Trans.* **1995**, 707.
(35) For example, see: Darensbourg, D. J.; Frost, B. J.; Larkins, D. L. *Inorg. Chem.* **2001**, *40*, 1993.
(36) Chisholm, M. H.; Extine, M. W. *J. Am. Chem. Soc.* **1977**, *99*, 782, 792.
(37) We have reported similar spontaneous reduction of Fe(III) complexes of polypyridine ligands in acetonitrile solvent. See: Patra, A. K.; Olmstead, M. M.; Mascharak, P. K. *Inorg. Chem.* **2002**, *41*, 5403.
(38) Chum, H. L.; Koran, D.; Osteryoung, R. A. *J. Am. Chem. Soc.* **1978**, *100*, 310.
(39) Maturano, M. D.; Bongibault, V.; Willson, M.; Klaébé, A.; Fournier, D. *Tetrahedron* **1997**, *53*, 17241.
(40) Wedemeyer-Exl, C.; Darbre, T.; Keese, R. *Helv. Chim. Acta* **1999**, *82*, 1173.
(41) Kersting, B. *Angew. Chem., Int. Ed.* **2001**, *40*, 3988.
(42) Presence of *N*-methyl imidazolium ion in the reaction mixture (Scheme 2) possibly makes the transfer of methyl group more facile at this step.
(43) One reviewer has suggested that a methyl transfer to bridging oxygen could first produce a methoxy-bridged diiron(III) species which in turn could react with CO_2 to afford the methyl carbonato complex **5**. In absence of detailed studies, this remains as another viable mechanism at this time.
(44) Kato, M.; Ito, T. *Inorg. Chem.* **1985**, *24*, 509.
(45) Pavlishchuk, V.; Birkelbach, F.; Weyhermuller, T.; Wieghardt, K.; Chaudhuri, P. *Inorg. Chem.* **2002**, *41*, 4405.

In conclusion, this work has shown that a simple (μ-oxo)(μ-carboxylato)diiron(III) core could be synthesized with simple N-donors such as *N*-MeIm. The mono(μ-carboxylato) complex is formed readily either via CO_2 fixation or addition of carboxylates to the reaction mixtures. The stability of the bis(μ-carboxylato) species is, however, low in this case, and only the very stable triiron carboxylato cluster is isolated from these reactions. We would also like to emphasize the fact that the *N*-MeIm/(μ-oxo)diiron(III) combination appears to have the ability to fix CO_2 into HCO_2^- or HCO_3^- depending on the concentration of CO_2.

Acknowledgment. This work was supported by grants from the National Science Foundation (CHE-9818492) and the National Institute of Health (GM 61636). The Bruker SMART 1000 diffractometer was funded in part by an NSF Instrumentation Grant CHE-9808259.

Supporting Information Available: Crystallographic data (excluding structure factors) for **1**, **3**·2THF, **4**·THF, **5**·0.5*N*-MeIm·THF, and **6**·2.5THF including positional parameters, thermal parameters, and bond distances and angles in CIF format. This material is available free of charge via the Internet at http://pubs.acs.org.

IC0206140